The Effect of Cell Size and Surface Roughness on the Compressive Properties of ABS Lattice Structures Fabricated by Fused Deposition Modeling

L. Mason and M. C. Leu

Department of Mechanical and Aerospace Engineering, Missouri University of Science and Technology, Rolla, MO 65409

Abstract

Researchers looking to improve the surface roughness of acrylonitrile butadiene styrene (ABS) parts fabricated by fused deposition modeling (FDM) have determined that acetone smoothing not only achieves improved surface roughness but increases compressive strength as well. However, the sensitivity of ABS parts to acetone smoothing has not been explored. In this study we investigated FDM-fabricated ABS lattice structures of various cell sizes subjected to cold acetone vapor smoothing to determine the combined effect of cell size and acetone smoothing on the compressive properties of the lattice structures. The acetone-smoothed specimens performed better than the as-built specimens in both compression modulus and maximum load, and there was a decrease in those compressive properties with decreasing cell size. The difference between as-built and acetone-smoothed specimens was found to increase with decreasing cell size for the maximum load.

Introduction

Fused deposition modeling (FDM) is a type of additive manufacturing (AM), or 3D printing, where plastic filament is heated and extruded through a nozzle to build up layers of a 3D part. AM has the capability to quickly create parts with complex geometries that are not possible using traditional methods of manufacturing. This capability has been used in automotive, aerospace, and medical fields to create lightweight designs for many applications. These lightweight designs often incorporate lattice structure elements within them, so it is important to understand as much as possible about lattice structures and how they function in order to use them most efficiently.

Lattice structures are engineered to resemble foams with specific properties, but they are known for generally having an excellent strength-to-weight ratio, and a high surface-area-to-volume ratio. The relative density of a lattice structure, or the ratio of material volume to the total volume the lattice structure occupies, is known as “the single most important structural characteristic” of a lattice structure [1]. As such, relative density has been extensively researched by many academicians. In this study, the relative density is kept constant, and another structural characteristic is studied: cell size.

To the best of our knowledge, no journal articles have been published on the effects of varying cell size of FDM lattice structures while keeping the relative density constant. For open-cell alumina foam, the relative elastic modulus does not change with different cell sizes, but the strut strength decreases with increasing cell size [2]. For body-centered cubic SLM Ti-6Al-4V, the relative elastic modulus and tensile strength decrease with increasing cell size [3]. For gyroid

SLM 316L stainless steel, the elastic modulus and compression yield strength decrease with increasing cell size [4]. For gyroid DMLS AlSi10Mg, compression strength and microhardness decrease with increasing cell size [5]. Many mechanical properties have been maximized by decreasing the unit cell size for metal AM lattice structures, but we do not know if this holds true for FDM fabricated lattice structures.

Postprocessing is an important step in many manufacturing processes, but it is especially important for additive manufacturing. Nearly all AM methods create parts with a high surface roughness, no matter the material. This high surface roughness leads to stress concentrations and is structurally inefficient. Researchers looking to improve the surface roughness of acrylonitrile butadiene styrene (ABS) parts fabricated by FDM have determined that acetone smoothing not only achieves improved surface roughness but increases compressive strength as well [6], [7]. This could be very beneficial to lattice structures, which are known for already having an excellent strength-to-weight ratio. Improving the compressive strength of ABS lattice structures even further using acetone smoothing could expand applications for plastic lattice structures and improve their uses across the board.

Postprocessing of metal AM lattice structures has already gained attention to improve the surface roughness of the lattice structures. Metal AM structures can be polished using chemical etching when conventional methods such as machining or blasting are not possible, as is the case with lattice structures. Ti-6Al-4V can be etched using an aqueous solution of hydrofluoric acid (HF) and nitric acid (HNO_3), which is a subtractive process that takes off an outer layer of material. This postprocessing method typically takes 30 minutes to a few hours to complete and improves the stiffness-to-density ratio [8], [9].

Smoothing of ABS parts using acetone is done using highly varying approaches that do not all agree on the same procedures for the "best" outcome. There are two main methods of acetone smoothing: submerging the part in a bath of acetone and subjecting the part to acetone vapors. Acetone bath smoothing is the fastest method, as it involves simply submerging the part in acetone for a few minutes. Submerging a part for 3-7 minutes significantly increases the ductility of the ABS and degrades the tensile strength of the part according to Jayanth et al [10]. Gautam et al. tested kagome lattice structures that had been smoothed using acetone baths, and they found that smoothing increased the compression strength and stiffness, and determined that 5 minutes is the best time for acetone bath smoothing [7].

Acetone vapor smoothing can be done using hot or cold vapors. Hot acetone vapor smoothing takes a few minutes, but the acetone is heated to release the vapors quickly. Hot acetone vapor has been known to increase the compressive strength of ABS after smoothing for 5, 7.5, and 10 minutes, although the 5 minutes smoothing withstood the highest compression force [6]. According to Lalehpour et al. [11], three hot vapor baths of 15 s each is the best way to smooth an ABS part to get the best surface roughness.

Cold acetone vapor smoothing works through evaporation and therefore takes more time, usually one or more hours, but is much safer than hot acetone vapor smoothing due to acetone's high flammability. Cold acetone vapor smoothing has not been widely reported in academic literature. One study was found that used cold acetone vapor smoothing. Zhang et al. [12] used

varying amounts of acetone poured on paper tissues and lined inside a beaker to smooth ABS parts for 30 minutes. The hobby community, however, seems to mainly use cold acetone smoothing to post-process their ABS parts. The cold acetone vapor smoothing method used in our study was based off of an article written by Susi Woods on the website rigid.ink [13].

In this study, FDM-fabricated ABS lattice structures of various cell sizes subjected to cold acetone vapor smoothing were investigated to determine the combined effect of cell size and acetone smoothing on the compressive properties of the lattice structures. The acetone-smoothed specimens performed better than the as-built specimens in both compression modulus and maximum load, and there was a decrease in those properties with decreasing cell size. The difference between as-built and acetone-smoothed specimens was found to increase with decreasing cell size for the maximum load.

Methods

Lattice Structure Design

The unit cell structure was a macro body-centered cubic (BCC) pattern with struts connecting the center to all eight corners of the unit cell cube. The BCC pattern was chosen because it is a commonly used lattice structure that requires no support material to print. The relative density of about 10.5% and specimen size of a 76.2 mm (3 in.) cube were kept constant. The lattice structures were created using the nTopology Element software. A 76.2 mm cube in STL format was imported into the Element software, and the lattice was generated using the cube vertex centroid rule. The struts were then thickened to have a uniform diameter, and a mesh of the lattice structure was generated and exported as an STL file.

The parameters of the lattice structures are shown in Table 1. The diameters of the struts were designed to be even multiples of the raster width of 0.508 mm (0.02 in.) so that the layers could be concentric ovals. This was done to minimize gaps and excess material in each layer and to maximize layer stability. The smallest strut diameter possible using this method was 1.016 mm (0.04 in.). The smallest cell size was then chosen to be 6.35 mm (0.25 in.) because that was an easily scaled size and it gave a reasonable relative density of about 10%. The cell size was then doubled, tripled, and quadrupled to obtain the 12.70 mm (0.50 in.), 19.05 mm (0.75 in.), and 25.40 mm (1.00 in.) cell sizes. The smallest overall specimen size that would allow for whole unit cells throughout all the specimens was a 76.2 mm (3 in.) cube.

Differences in the relative density, dimensions, and volume of material used are mainly due to the rounded caps on the outside corners and ends of the lattice structures. These caps ensured that the lattice structures performed appropriately and that the outer corners were not unnecessarily weakened, but they did add more material to the specimens for the larger cell sizes. The volume and dimensions were taken from the Stratasys Insight software that was used to slice and generate toolpaths for printing the lattice structures.

Table 1: Lattice Structure Parameters

Lattice cells	3x3x3	4x4x4	6x6x6	12x12x12
Cell Size (in.)	1.00	0.75	0.50	0.25
Cell Size (mm)	25.40	19.05	12.70	6.35
Volume (in.^3)	3.493	3.208	3.182	2.904
Volume (mm^3)	57240	52570	52144	47588
Dimensions (in.)	3.192	3.132	3.088	3.035
Dimensions (mm)	81.072	79.548	78.435	77.086
Strut Diameter (in.)	0.16	0.12	0.08	0.04
Strut Diameter (mm)	4.064	3.048	2.032	1.016
Relative Density	10.74%	10.44%	10.80%	10.39%

Manufacturing

Figure 1 shows pictures of one replication. In this study, data from six replications were analyzed. There were four cell sizes and two relative roughness values: as-built and acetone-smoothed, for a total of eight treatment combinations. Each replication of lattice structures included all eight treatment combinations, for a total of 48 specimens. All specimens were printed using the fused deposition modeling (FDM) process on a Stratasys Fortus 400mc using white ABS-M30. One full replication was printed at a time, and the lattice structures were randomly placed in the positions shown in Figure 2 in the 355.6 x 406.4 x 355.6 mm^3 (14 x 16 x 14 $inch^3$) build volume to account for possible differences in placement within the build chamber.

The rounded feet of the lattice structures did not reliably stick to the support material raft that is automatically printed under every print in the Fortus. This made necessary some reinforcing support material under the first struts of every specimen to ensure that the lattice structures printed reliably and well. The support structure used was designed to allow the lattice structures to be broken off the support with minimal harm. The only problem that came of the support structure was the loss of some corner struts on the 6.35 mm specimens. The corner struts are the most fragile, especially on the smallest cell size, since they are only connected to the structure on one end. Figure 1d shows only one surviving corner strut out of the four visible lower corners of the 6.35 mm specimens.

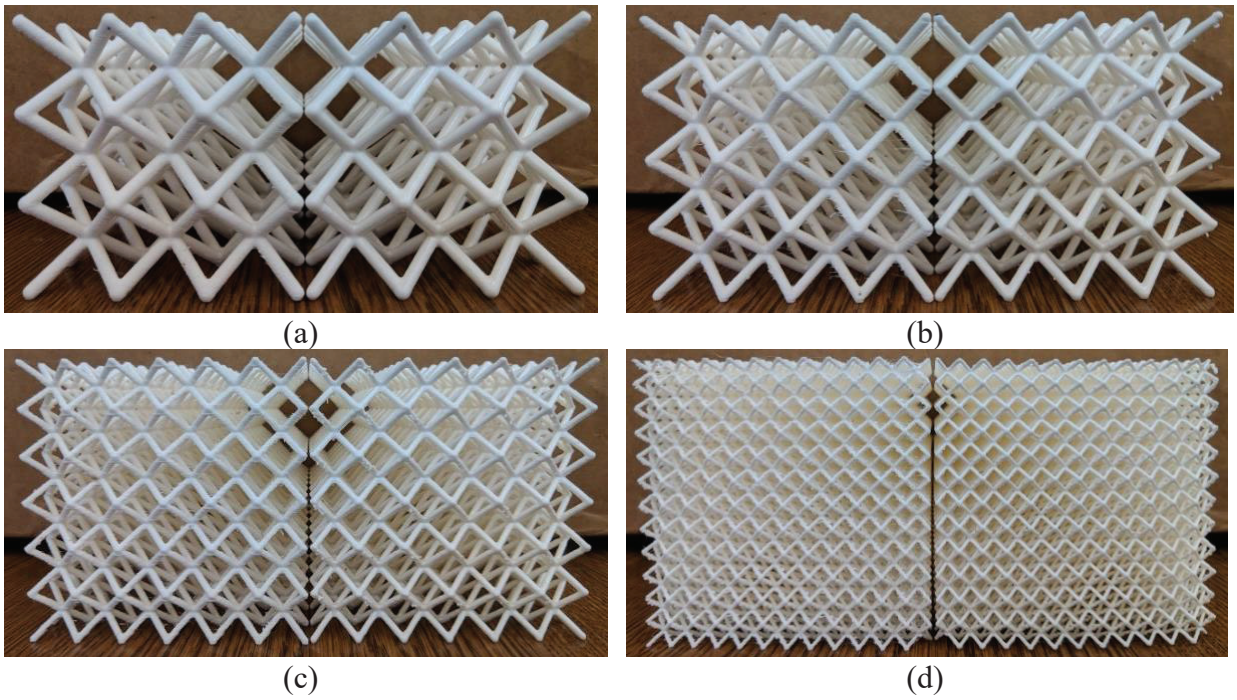

Figure 1: Pictures of one full replication with 8 specimens, with as-built (left) and acetone-smoothed (right) specimens of cell size (a) 25.40mm (1.00 in), (b) 19.05 mm (0.75 in), (c) 12.70 mm (0.50 in), and (d) 6.35 mm (0.25 in)

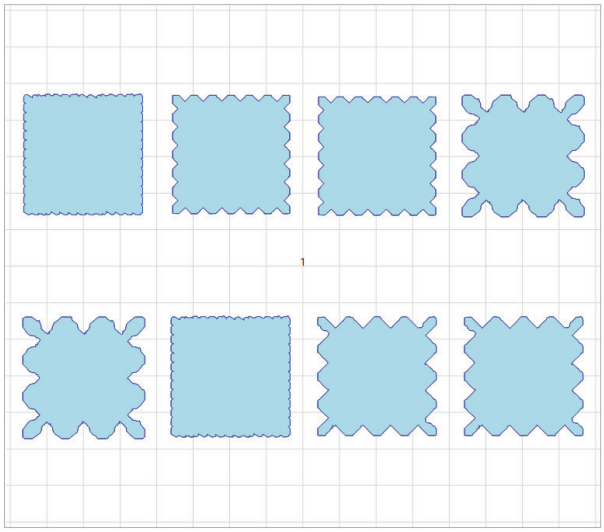

Figure 2: Specimen positions within Fortus 400mc build volume, replication 1

Acetone Smoothing

Half of the specimens, one of each cell size in each replication, were subjected to cold acetone vapor smoothing. All four specimens from one replication were smoothed at the same time to facilitate equality within each replication. The specimens were smoothed in a 9 L polypropylene container on top of a polypropylene stage, shown in Figure 3, all within a fume

hood. The stage held one specimen on each corner and had slots machined in between the specimens to allow for improved airflow. A fan underneath the stage circulated the vapors within the container by forcing air down through the stage slots and out and around the specimens. The vapors originated from acetone-soaked paper towels lining the bottom of the container. Each replication was smoothed for 50 minutes using 80 mL of acetone.

The smoothing time and amount of acetone to use were determined by testing specimens that failed to print correctly, such as ones that were interrupted mid-print or ones that did not stick to the printing bed. First, the amount of acetone was determined by testing in increments of 20 mL and checking every half an hour for two hours; 20 mL did nothing visible for two hours, 40 mL made the specimens sort of glossy, 60 mL started smoothing the specimens but did not finish in two hours, and 80 mL had warped the specimens in an hour and a half. The amount chosen was 80 mL, and then the time to smooth the specimens was narrowed. The specimens were checked every 5 minutes until the smallest lattice structure just started to warp at one hour. Fifty minutes was then chosen as the amount of time to smooth the specimens. The purpose behind this stopping point was to give the acetone as much time as possible to smooth the parts without causing any warping due to loss of structural integrity.

When placing the specimens into the container and removing them from the container, only the polypropylene stage was touched. The specimens were placed on the stage and then the stage was lowered into the container on top of the fan and the lid of the container was closed and sealed. The specimens were removed in a reverse fashion once the smoothing was complete. All specimens were allowed to dry for at least twelve hours in the fume hood before handling. Handling an ABS part directly after acetone smoothing can introduce surface deformations and dust particles that would embed themselves into the malleable surface permanently. At least two weeks passed in between acetone smoothing the specimens and compression testing the specimens to ensure that the ABS had completely resolidified. The mass of each specimen was recorded before and after smoothing.

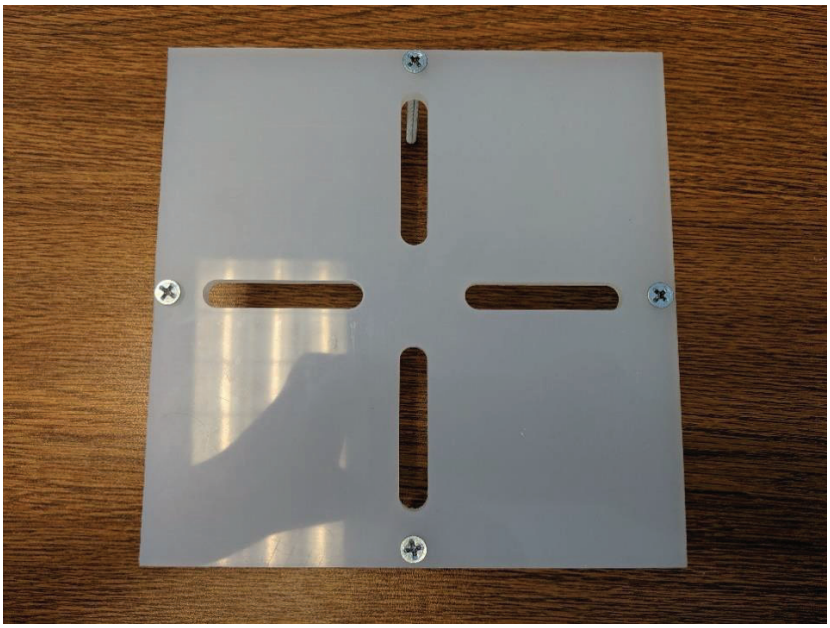

Figure 3: Polypropylene stage for cold acetone smoothing process

Compression Testing and Surface Roughness Measurement

The lattice structures were compression tested using an Instron 5969 Universal Testing System at a rate of 7.5 mm/min until catastrophic failure. After the specimens were compression tested, an outside edge strut of each specimen was broken off for surface roughness measurement with a profilometer. The profilometer used was a KLA-Tencor P-17, which has a stage with locating holes. To reliably position the broken struts on the stage, a locating fixture, shown in Figure 4, was created and printed from ivory PLA on a Prusa i3 MK2 printer. The two locating pegs on the bottom of the fixture sit in the locating holes on the profilometer stage, while the lattice structure strut sits along the groove on the top of the fixture. Since the strut is cylindrical, the groove ensures that the struts are always aligned with the x-axis of the profilometer. The end of the groove (shown on the left side of Figure 4b) that is in between the two locating pegs serves as a locating point to push the lattice structure strut up against.

(a) (b)

Figure 4: Locating fixture for profilometer measurements: (a) bottom with locating pegs, (b) top with locating groove for lattice structure struts

One additional strut from each specimen in the first replication was taken to look at the cross sections of the struts. The struts were broken off each specimen after compression testing and set in epoxy. In order to stand the struts up in the epoxy mold, the struts were grouped together on top of a bead of epoxy, and another bead of epoxy was dropped onto the cluster of struts and allowed to harden. Then, epoxy was poured around the cluster to complete the mold. The epoxy-set cluster of struts was then polished following the methods described in *Metallography* by G. Vander Voort [14] using the following steps, resulting in the cross sections of all eight specimens shown in Figure 5:

1) 400 grit SiC paper at 200 rpm with 5 lbs of force for 45 s increments until desired region of specimens was reached
2) 600 grit SiC paper at 200 rpm with 3 lbs of force for 45 s
3) 800 grit SiC paper at 200 rpm with 3 lbs of force for 45 s
4) 1200 grit SiC paper at 200 rpm with 3 lbs of force for 45 s
5) 9 µm water-based diamond suspension at 150 rpm with 3 lbs of force for 5 min
6) 3 µm water-based diamond suspension at 120 rpm with 3 lbs of force for 3 min
7) 1 µm water-based diamond suspension at 120 rpm with 3 lbs of force for 3 min

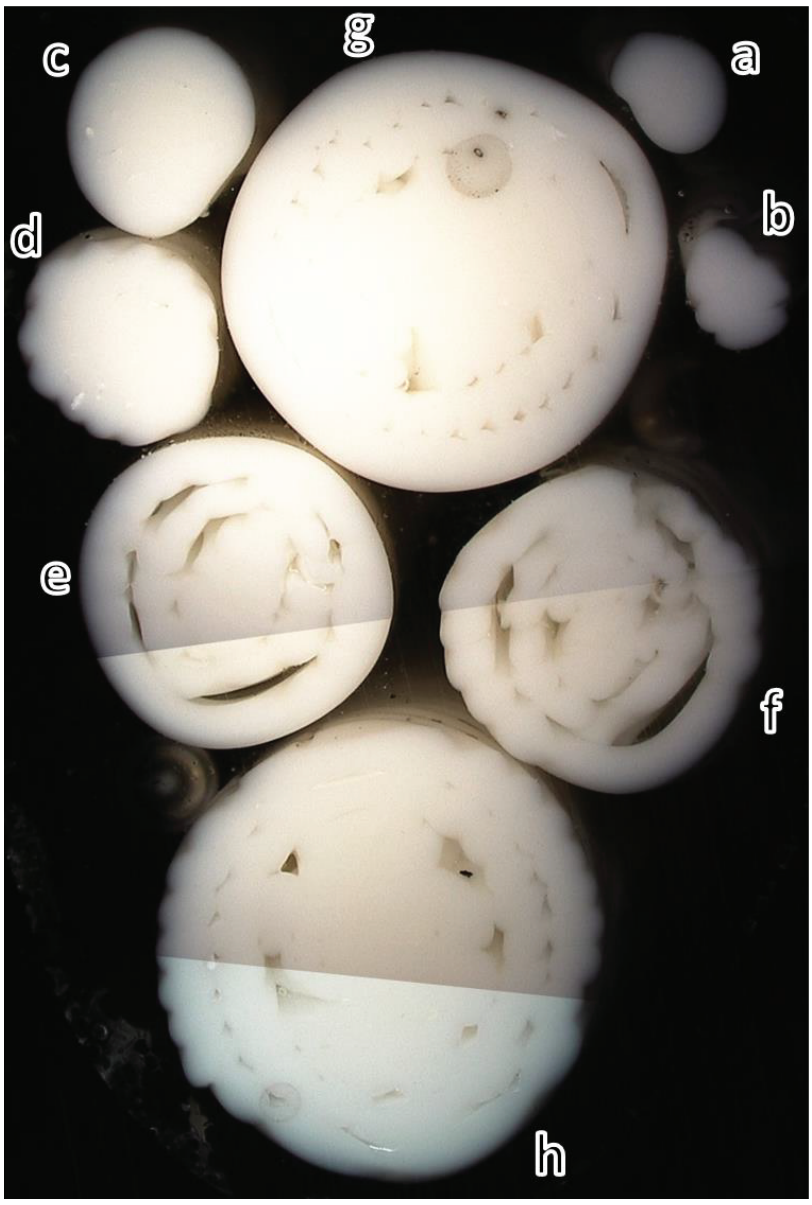

Figure 5: Cross sections of one strut of each treatment combination from replication 1, with (a) acetone-smoothed 6.35 mm (0.25 inch) cell size, (b) as-built 6.35 mm (0.25 inch) cell size, (c) acetone-smoothed 12.70 mm (0.50 inch) cell size, (d) as-built 12.70 mm (0.50 inch) cell size, (e) acetone-smoothed 19.05 mm (0.75 inch) cell size, (f) as-built 19.05 mm (0.75 inch) cell size, (g) acetone-smoothed 25.40 mm (1.00 inch) cell size, (h) as-built 25.40 mm (1.00 inch) cell size

Results and Discussion

The mass of each specimen was recorded before and after smoothing, the averages of which are shown in Table 2. All the acetone-smoothed specimens increased in mass, but the increase was no more than 5%. There is a definite correlation between the increase in mass and an increase in surface area. The smallest cell size, 6.35 mm, is not the structure with the least mass. This is due to the extra material that was deposited as strands that connected different struts within the same layer and potential further excess material from printing inconsistencies.

Table 2: Average mass before and after acetone smoothing

Cell Size (in)	Cell Size (mm)	As-Built Mass (g)	Std. Dev.	Acetone-Smoothed Mass (g)	Std. Dev.	Difference (g)	Difference (%)
1.00	**25.40**	55.519	0.153	56.450	0.382	0.930	1.675
0.75	**19.05**	48.629	0.126	49.643	0.391	1.014	2.084
0.50	**12.70**	45.677	0.169	47.192	0.507	1.515	3.315
0.25	**6.35**	49.057	0.144	50.958	0.558	1.901	3.874

The cross sections shown in Figure 5 give some insight into how far the cold acetone vapors penetrate the struts. The struts were built on the diagonal, so there are multiple layers shown in the cross sections. In cross sections e-h, there are two outer rings of material composed by the first and second contours of each layer. A contour is known as the outline of each layer in FDM, counted from the outside of the layer towards the middle, and in this study, there is a maximum of two contours per layer. Only the first contour (the outermost) is affected by the acetone smoothing, and even then, not completely. The ridges on the outer ring of material that can be seen in cross sections f and h are still present on the inside of the outer rings in cross sections e and g. This implies that the acetone vapors were not able to penetrate the full thickness of the outer ring of material.

The surface roughness of one strut broken off of each specimen was measured using a profilometer, and the results are shown in Figure 6. The profilometer could not record an amplitude of greater than 163.5 microns in the positive or negative direction, which limited the areas of the struts that could be measured. There were sections of each strut that were within these limitations, but the sections that were measured typically had to be the smoothest and most consistent sections on the struts. The Ra values that were obtained are therefore a lower bound estimate instead of an average estimate for the surface roughness of the lattice structures. This being said, the average values that were measured from these specimens do indicate that cold acetone smoothing decreases the surface roughness of ABS specimens fabricated by FDM, as expected. This can also be seen in the cross sections shown in Figure 5.

The lattice structures with the two largest cell sizes have the smallest surface roughness values, and of those, the as-built specimens are extremely similar. The surface roughness of the lattice structures increases for the two smaller cell sizes for both as-built and acetone-smoothed specimens. The range of Ra values for the acetone-smoothed specimens increases significantly as the cell size decreases. The average surface roughness of the smallest cell size is by far the highest at 36.9 microns. This high surface roughness can be attributed to the stability of the printing process. Figure 7 shows an up-close visual comparison between as-built and acetone-smoothed specimens of each cell size, where it is shown that the uniformity of the struts decreases with cell size. This is a symptom of a decreasing number of layers and smaller, less-uniform layers. Smaller layers are not printed as accurately or consistently as larger layers because the printing inconsistencies are amplified for smaller layers and make more of a difference for smaller geometries.

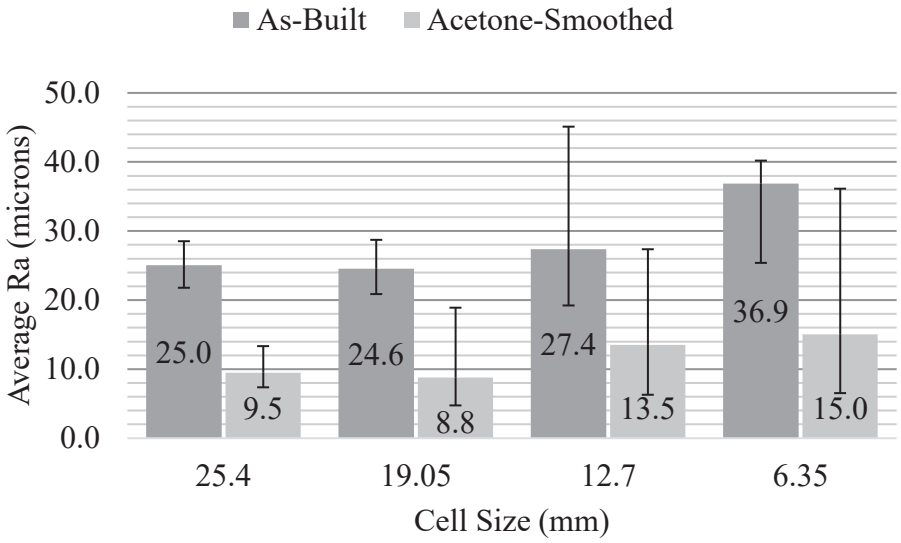

Figure 6: Average surface roughness Ra vs. cell size. The error bars indicate maximum and minimum values

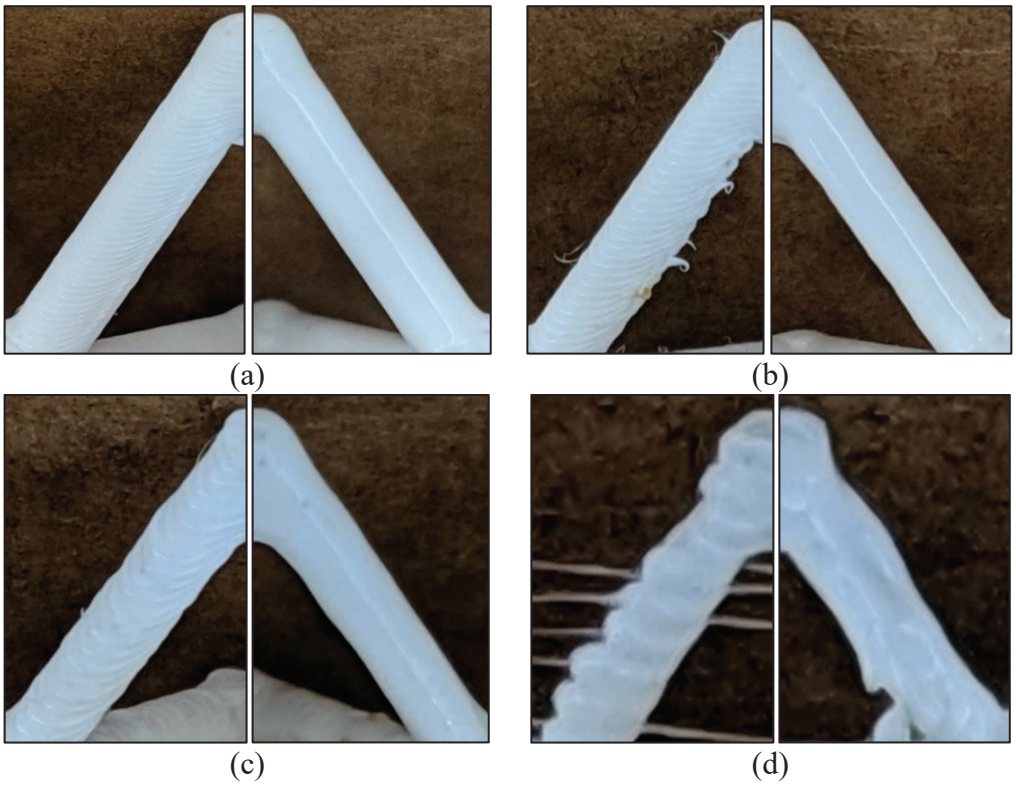

Figure 7: Visual comparison between as-built (left) and acetone-smoothed (right) specimens of (a) 25.40 mm (1.00 in), (b) 19.05 mm (0.75 in), (c) 12.70 mm (0.50 in), and (d) 6.35 mm (0.25 in) cell size

The elastic modulus of each specimen was calculated, and the average elastic modulus for each treatment combination is shown in Figure 8. The maximum load was recorded for each specimen, and the average maximum load for each treatment combination is shown in Figure 9. Most of the specimens broke along a perfect 45-degree angle, as expected. The compression results show a definite correlation between decreasing compressive properties and decreasing cell size. This was not expected as Yan et al. [4], [5] claims that the smaller cell sizes of metal lattice structures have better compressive properties than larger cell sizes. For metal AM, smaller cross-sectional areas mean shorter scan distances which leads to faster scanning of adjacent sections and increases the temperature of the smaller scanned area. Increased temperature gives the right conditions for higher compression strength and modulus.

Conversely, smaller FDM layers are not printed as accurately or consistently as larger FDM layers. For smaller layers, the machine must move in shorter, faster bursts which introduces printing inconsistencies due to machine backlash and shaking. For larger layers, it takes more time, the movements are smoother, and the direction changes are more spread out. Therefore, the decreasing compressive properties with decreasing cell size in this study can be attributed to the decreasing uniformity and quality of the struts.

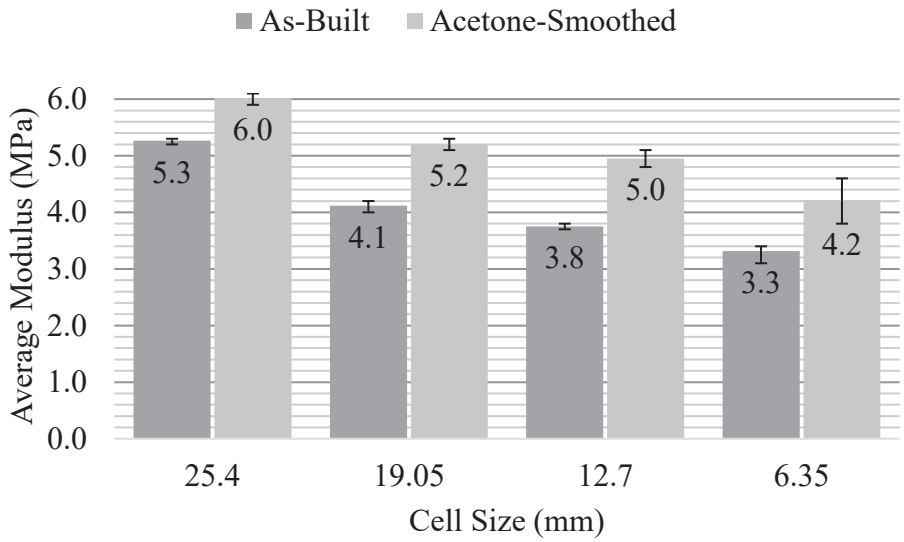

Figure 8: Average elastic modulus vs. cell size. The error bars indicate maximum and minimum values

Lattice structures are known for their high strength-to-weight ratio, also called specific strength or strength-to-mass ratio. The strength-to-weight ratio is calculated by dividing the material's strength by its density. The material's strength is the maximum load the lattice structure could bear divided by the cross-sectional area of the structure as a whole, which in this case is 5806.44 mm^2, or 9 $in.^2$. The material's density is the mass of the lattice structure in kilograms divided by the volume of the structure as a whole, which in this case is 442451 mm^3, or 27 $in.^3$. Specific strength therefore has units of $Pa*m^3/kg$ or N*m/kg. The calculated average strength-to-weight ratios are shown in Figure 10. This graph is similar to the maximum load graph in that the difference between as-built and acetone-smoothed specimens increases with decreasing cell size, but it is interesting to note that the smallest cell size had a much lower

strength-to-weight ratio than the others. This result for the 6.35 mm cell size was a combination of the lowest maximum load and a mass on par with the 19.05 mm cell size. The highest strength-to-weight ratio came from the acetone-smoothed 12.70 mm cell size lattice structure. The 12.70 mm cell size lattice structure had a mid-range maximum load and the smallest mass of all the cell sizes, which combined to give it the best acetone-smoothed strength-to-weight ratio.

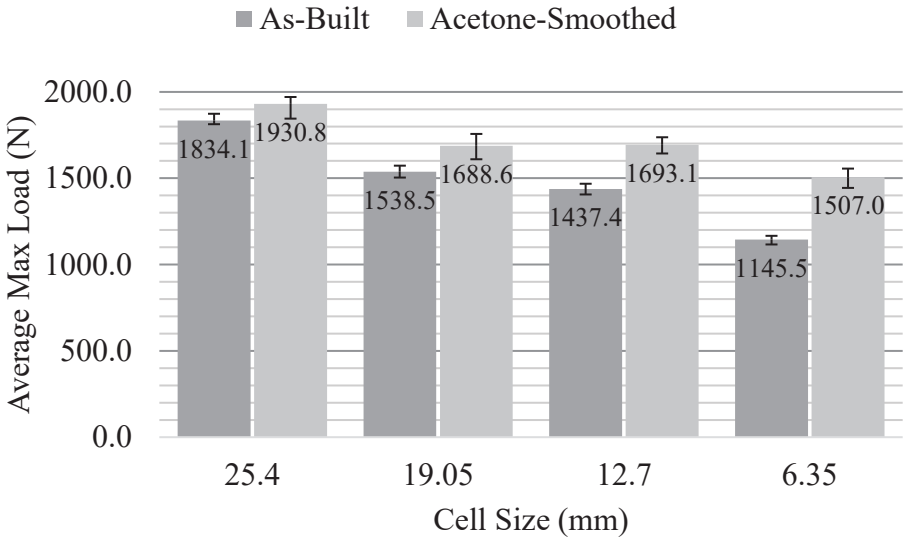

Figure 9: Average maximum load vs. cell size. The error bars indicate maximum and minimum values

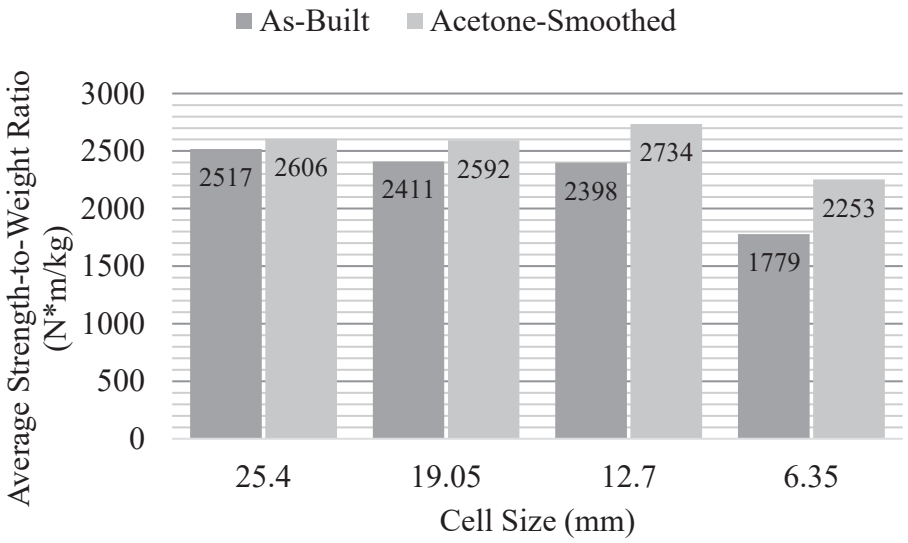

Figure 10: Average strength-to-weight ratio vs. cell size

There was an increase in ductility from the as-built specimens to the acetone-smoothed specimens. All the as-built specimens made clean breaks when they failed, but some of the acetone-smoothed 25.40 mm (1.00 in.) cell size specimens did not break apart completely when they failed. These specimens fractured and bent a diagonal plane of struts at both joints, but they

were still held together by the outer layer of material. The outer layer was the material that was most affected by the acetone and exhibited significantly more ductile behavior, while the inner layers were not as affected by the acetone and behaved similarly to the as-built specimens.

It can be observed that subjecting the lattice structures to acetone vapor smoothing increases the compressive properties of the lattice structures in general. Both the elastic modulus and maximum load consistently increased from as-built to acetone-smoothed, with little to no overlap. This can be attributed at least in part to the near-elimination of stress concentrations in the acetone-smoothed specimens. Acetone smoothing also increased the effective diameter of the struts by filling in the stress concentrations and indentations where the layers meet. The effective diameter in this case is the smallest diameter of the strut, which happens where two layers meet. The diameter of the contact between the two layers is considered the effective diameter because any material that extends beyond that would not take any of the load held by the strut. After acetone smoothing, the area of contact between two layers is increased by taking the extra material that did not contribute to taking the load before and spreading it evenly along the strut, therefore increasing the effective diameter and using more of the material to carry the load. This increases the bond between layers by increasing the contact area between them.

Table 3 shows the percent difference between the average maximum load results for as-built and acetone-smoothed specimens. It is very apparent that the difference in average maximum load increases as the cell size decreases, meaning that the acetone smoothing had a larger impact on the smaller cell sizes than on the larger cell sizes. This trend is in part caused by the increased uniformity of the struts from acetone smoothing, especially for the smaller cell sizes, and the increased cohesion between layers due to the increased effective diameter.

Table 3: Percent difference between average values of maximum load

Cell Size (mm)	**25.40**	**19.05**	**12.70**	**6.35**
Avg. Max Load	5.1%	9.3%	16.3%	27.3%

An analysis of variance (ANOVA) was run on each set of compression results to determine if the response from the two combined factors, cell size and surface roughness, was additive or interactive. For either model, factor *a* creates a certain independent response, *A*, and factor *b* creates another independent response, *B*. The additive model's response is just *A*+*B*, meaning adding the factors' separate responses together results in the combined response. The interactive model adds another variable to the combined response equation, called the interaction effect variable, *C*, making the response equation *A*+*B*+*C*. This interaction effect variable represents the response from the non-additive relationship between factors *a* and *b*. A two-factor ANOVA simply determines if the model is interactive or additive, and it does not determine what the interactive effect is. The ANOVA results shown in Table 4 indicate that the interaction between the cell size and qualitative surface roughness is significant for the elastic modulus and the maximum load because the p-value is less than 0.05, meaning the model is interactive for both of those responses. This interactive model can especially be seen in Figure 9, where the increase in maximum load from as-built to acetone-smoothed changes based on the cell size. If

this was an additive model, acetone smoothing the specimens would have increased the maximum load by the same amount no matter the cell size.

Table 4: ANOVA results

Data	Interaction P-value
Modulus	0.0002
Max Load	< 0.0001

Conclusions

Lattice structures of four different cell sizes, half of which were exposed to cold acetone vapor smoothing, were tested in compression to determine the combined effect of cell size and acetone smoothing. The difference between as-built and acetone-smoothed specimens was found to increase with decreasing cell size for the maximum load. This trend was caused by the increased uniformity of the struts from acetone smoothing, especially for the smaller cell sizes, and the increased cohesion between layers due to the acetone fusing the layers together on the outside. The acetone-smoothed specimens performed better than the as-built specimens in both elastic modulus and maximum load, and there was a decrease in those compressive properties with decreasing cell size. The increase in compressive properties for the acetone-smoothed specimens can be attributed at least in part to the reduction of stress concentrations and the increase in effective diameter. The decreasing compressive properties with decreasing cell size can be attributed to the decreasing uniformity and quality of the struts. There was also an increase in ductility from the as-built specimens to the acetone-smoothed specimens in the outer layer of material. Overall, the acetone smoothing affected the compressive properties of the smaller cell sizes more significantly than the larger cell sizes. It was determined through an ANOVA test that the two factors, cell size and qualitative surface roughness, were not purely additive and that they interacted to give unique results. Therefore, there exists an optimum combination of cell size and surface roughness that gives the best response depending on the application.

References

[1] L. J. Gibson and M. F. Ashby, *Cellular Solids: Structure and Properties*, Second Edi. Cambridge University Press, 1999.

[2] R. Brezny and D. J. Green, “The effect of cell size on the mechanical behavior of cellular materials,” *Acta Metall. Mater.*, vol. 38, no. 12, pp. 2517–2526, 1990.

[3] I. Maskery, A.O. Aremu, M. Simonelli, C. Tuck, R.D. Wildman, I.A. Ashcroft, and R.J.M. Hague , “Mechanical Properties of Ti-6Al-4V Selectively Laser Melted Parts with Body-Centred-Cubic Lattices of Varying cell size,” *Exp. Mech.*, vol. 55, no. 7, pp. 1261–1272, 2015.

[4] C. Yan, L. Hao, A. Hussein, and D. Raymont, “Evaluations of cellular lattice structures

manufactured using selective laser melting," *Int. J. Mach. Tools Manuf.*, vol. 62, pp. 32–38, 2012.

[5] C. Yan, L. Hao, A. Hussein, P. Young, J. Huang, and W. Zhu, "Microstructure and mechanical properties of aluminium alloy cellular lattice structures manufactured by direct metal laser sintering," *Mater. Sci. Eng. A*, vol. 628, pp. 238–246, 2015.

[6] J. Beniak, P. Križan, Ľ. Šooš, and M. Matúš, "Roughness and compressive strength of FDM 3D printed specimens affected by acetone vapour treatment," *IOP Conf. Ser. Mater. Sci. Eng.*, vol. 297, p. 012018, 2018.

[7] R. Gautam, S. Idapalapati, and S. Feih, "Printing and characterisation of Kagome lattice structures by fused deposition modelling," *Mater. Des.*, vol. 137, pp. 266–275, 2018.

[8] P. Lhuissier, C. de Formanoir, G. Martin, R. Dendievel, and S. Godet, "Geometrical control of lattice structures produced by EBM through chemical etching: Investigations at the scale of individual struts," *Mater. Des.*, vol. 110, pp. 485–493, 2016.

[9] C. de Formanoir, M. Suard, R. Dendievel, G. Martin, and S. Godet, "Improving the mechanical efficiency of electron beam melted titanium lattice structures by chemical etching," *Addit. Manuf.*, vol. 11, pp. 71–76, 2016.

[10] N. Jayanth, P. Senthil, and C. Prakash, "Effect of chemical treatment on tensile strength and surface roughness of 3D-printed ABS using the FDM process," *Virtual Phys. Prototyp.*, vol. 0, no. 0, pp. 1–9, 2018.

[11] A. Lalehpour, C. Janeteas, and A. Barari, "Surface roughness of FDM parts after post-processing with acetone vapor bath smoothing process," *Int. J. Adv. Manuf. Technol.*, vol. 95, no. 1–4, pp. 1505–1520, 2018.

[12] S. U. Zhang, J. Han, and H. W. Kang, "Temperature-dependent mechanical properties of ABS parts fabricated by fused deposition modeling and vapor smoothing," *Int. J. Precis. Eng. Manuf.*, vol. 18, no. 5, pp. 763–769, 2017.

[13] S. Woods, "How To Easily Cold Acetone Vapour Smooth & Finish 3D Prints [Step by Step]," 2019. [Online]. Available: https://rigid.ink/blogs/news/acetone-vapor-smoothing. [Accessed: 31-May-2019].

[14] G. F. Vander Voort, *Metallography, principles and practice*. ASM International, 1999.